# Evidence of intrinsic exchange bias and its origin in spin-glass-like disordered $L_{0.5}Sr_{0.5}MnO_3$ manganites ($L$=Y, $Y_{0.5}Sm_{0.5}$, and $Y_{0.5}La_{0.5}$)

Shilpi Karmakar, S. Taran, Esa Bose, and B. K. Chaudhuri*
*Department of Solid State Physics, Indian Association for the Cultivation of Science, Kolkata 700032, India*

C. P. Sun, C. L. Huang, and H. D. Yang
*Department of Physics, Center for Nanoscience and Nanotechnology, National Sun Yat-Sen University, Kaohsiung 804, Taiwan*
(Received 16 July 2007; revised manuscript received 8 January 2008; published 7 April 2008)

Exchange-bias (EB) phenomena have been observed in the $L_{0.5}Sr_{0.5}MnO_3$ ($L$=Y, $Y_{0.5}Sm_{0.5}$, and $Y_{0.5}La_{0.5}$)-type manganites showing cluster-glass-like and spin-glass-like behavior. The field cooled magnetic hysteresis loops exhibit shifts both in the field and magnetization axes. The values of exchange field ($H_E$), coercivity ($H_C$), remanence asymmetry ($M_E$), and magnetic coercivity ($M_C$) of $L_{0.5}Sr_{0.5}MnO_3$ are found to depend strongly on temperature, measuring field, as well as strength of cooling field $H_{cool}$. $H_E$ increases sharply with the magnitude of $H_{cool}$ ($\leqslant$3 T), but for larger $H_{cool}$ ($>$3 T), it decreases due to the growth of the ferromagnetic cluster size. This observed behavior has been explained in terms of interfacial exchange coupling between coexisting ferromagnetic cluster glass and the disordered spin-glass-like phases, where the spin configurations are strongly affected by the cooling field strength. Below the spin and/or cluster glass freezing temperature ($T_f$), both $H_E$ and $M_E$ decrease exponentially with temperature. The value of $H_C$ increases almost exponentially with increasing magnetic-field step size ($\Delta H$). In addition, the observed training effect of the EB behavior has been explained well in terms of the existing relaxation model developed for other classical EB systems. In view of the use of manganites in spintronics, the present observation of EB-like shift even in the mixed valent polycrystalline manganites such as $L_{0.5}Sr_{0.5}MnO_3$ is of paramount importance.

DOI: 10.1103/PhysRevB.77.144409 PACS number(s): 75.47.Lx, 71.70.Gm, 75.50.Lk

## I. INTRODUCTION

Exchange interaction between ferromagnetic (FM) and antiferromagnetic (AFM) materials often leads to an interesting phenomenon called "exchange bias" (EB).[1,2] In a magnetic hysteresis loop, it manifests itself as a shift $H_E$ from zero field as well as an increase in loop width. As both these effects vanish at or close to the AFM Néel temperature $T_N$, they are attributed to the coupling of the FM and the AFM regions and/or layers. The EB effect has been found in different types of systems, viz., nanoparticles where the cores couple to the shells,[1–4] inhomogeneous spin glasses (SGs) where FM domains couple to AFM domains,[4] thin films consisting of bilayers[6] where a FM layer couples to an AFM layer, or in double superlattices where an artificial FM superlattice couples to an artificial AFM superlattice.[7] Spin-glass-like behavior is also found to be dominant in the surface or interface of exchange-biased nanoparticles,[3,8] and it has been suggested to be involved also with the interfacial coupling of AFM/FM bilayers.[8] Recently, Ali *et al.*[9] reported their observation of EB in Co/CuMn (FM/SG) bilayer metallic system, and it was suggested that EB properties of the FM/SG system, in terms of length scales and blocking temperature, differ from those of the usual AFM/FM exchanged biased systems.

Though various theoretical approaches on exchange-bias phenomena have been put forward,[1,8] clear understanding of the microscopic coupling mechanisms and quantitatively satisfactory model describing the systems are still missing. Uncompensated (UC) spins associated with the antiferromagnets or their interfaces have early been suggested to mediate the coupling between AFM and FM materials. For the thin film system, it has been shown that a part of these spins rotate when the FM layer is reversed, while another part is "pinned" in the bias direction.[10,11] "Pinning effects" in exchange-bias systems are not necessarily related to UC spins; they may also be due to a frozen state similar to a spin-glass state.[12] For a FM/AFM uniaxial system, only two energetically equivalent spin configurations exist for the AFM region and, following the field-cooling process, the exchange interaction with the FM phase selects one of the two. On the other hand, strong influence of the cooling field on the exchange-bias phenomenon may be expected for a spin-glass interface due to the multivalley energy structure and multiple equivalent spin configurations of the SG phase. Depending on the magnitude of the cooling field $H_{cool}$, applied above $T_f$ (spin freezing temperature), the magnetization of the ordered phase tends to align more and more in the field direction. As the temperature is lowered across $T_f$, a particular spin configuration of the SG phase will be selected through the exchange interaction with the ordered component. Thus, depending on the strength of $H_{cool}$, the degeneracy of the SG state can be reduced (actually, strong enough magnetic field can destroy the SG state entirely), which makes the SG system an interesting candidate for studying the EB effect in manganites both for fundamental and technological interests.

Recent research on the hole-doped perovskite manganites has drawn much attention, mainly due to the discovery of the colossal magnetoresistance (CMR) in them.[13] CMR materials show that the intrinsic phase separation plays a crucial role governing their complicated physical properties.[14] It has been recognized that the electronic phase diagram of CMR manganites is multicritical, involving competitions of spin,

 

charge or orbital, and lattice orders[15,16] leading to electronic phase separation and inhomogeneous electronic and magnetic ground states. At the same time, the significance of intrinsic disorder in manganites has also been recognized. For example, in $L_{1-x}Sr_xMnO_3$ ($x \sim 0.5$), $L$ and Sr ions can form an ordered or disordered structure causing a significant disordered effect.[17–19] This disorder can result in a glassy magnetic ground state and enhance fluctuation of the order competitions, i.e., between the charge-ordered–orbital-ordered states and ferromagnetic metal state, near the original bicritical point. Such fluctuations are amenable to an external magnetic field. It has been proposed that the phase separation in half-doped manganites can be in the form of FM clusters embedded in a nonmagnetic matrix with SG regions between them as interfaces.[20] Thus, the intrinsic phase separation leads to the FM/SG interfaces in cation size disordered manganites. As mentioned above, EB has been observed earlier in some other bilayered and core-shell systems containing FM/SG interfaces. Therefore, it is important to explore the existence of exchange bias in the intrinsically phase-separated cation disordered manganites, which are widely studied for spintronic device applications.[21]

In the present work, we report the existence of strong exchange bias in a typical manganite system viz., $L_{0.5}Sr_{0.5}MnO_3$ ($L$=Y, $Y_{0.5}La_{0.5}$, and $Y_{0.5}Sm_{0.5}$), showing spin-glass-like and/or cluster-glass-like behavior. A detailed investigation of the temperature, field, field step, and cycling effects of the EB properties has been made and the data have been analyzed with theoretical models to elucidate the origin and nature of the observed EB phenomena in these interesting mixed valent manganite samples.

## II. EXPERIMENT

The $L$ doped $L_{0.5}Sr_{0.5}MnO_3$ ($L$=Y, $Y_{0.5}Sm_{0.5}$, and $Y_{0.5}La_{0.5}$) samples were synthesized by standard solid state reaction method in air from their respective metal oxides (each of 99.9% or better purity) as starting materials. The initial mixture was preheated at several temperatures ranging from 873 to 1473 K with intermediate grindings. The resultant black powder of the respective samples were grounded, pressed into pellets and fired again in air at temperatures of 1473–1623 K for 24 h. A slow cooling procedure was employed to get better results. The annealing procedure was repeated two to three times with intermediate grindings. The structure and composition of the samples were checked by powder x-ray diffraction (XRD), scanning electron microscopy (SEM), and energy dispersive x-ray analysis measurements, respectively. Magnetization was measured by a superconducting quantum interference device (SQUID) magnetometer (Quantum Design magnetic properties measurement system at National Sun-Yat-Sen University, Taiwan).

## III. RESULTS AND DISCUSSION

### A. Characterization

Figures 1(a) and 1(b) represent x-ray diffraction patterns of the $L_{0.25}Sr_{0.5}MnO_3$ samples with $L$=Y and $La_{0.5}Y_{0.5}$, respectively. The XRD peaks can be well refined considering the orthorhombic structure (Table I) with space group *Pnma*. Fitting parameters such as atomic positions, etc., are found to be comparable to those of similar manganite samples.[22]

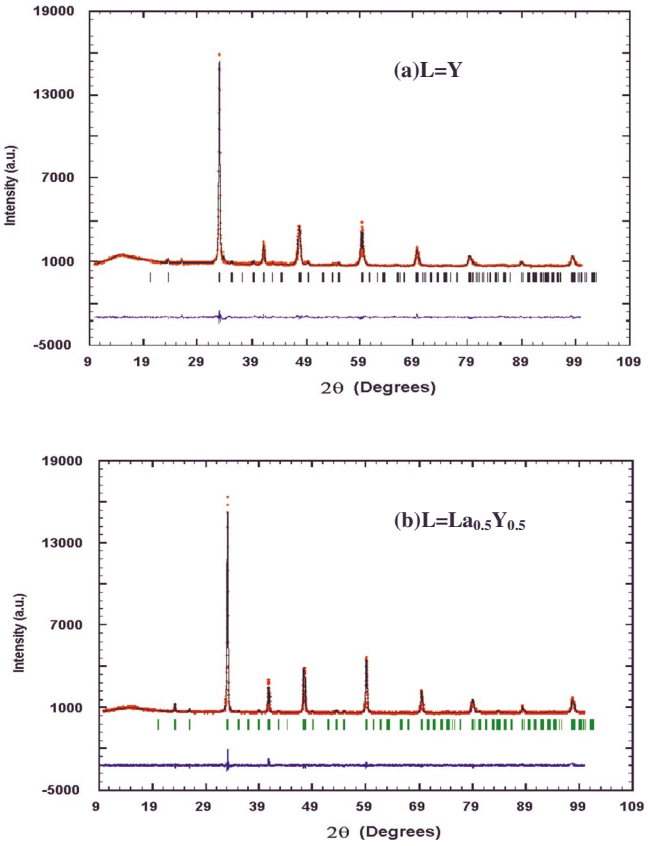


FIG. 1. (Color online) Room temperature XRD patterns for (a) $Y_{0.5}Sr_{0.5}MnO_3$ and (b) $La_{0.25}Y_{0.25}Sr_{0.5}MnO_3$ (square symbols and solid lines denote the experimental and calculated patterns, respectively). The vertical marker represents the calculated Bragg positions and the lower line shows the difference between the experimental and calculated pattern intensities.

It has been recently suggested that EB has a strong grain size dependence.[23] To confirm that the observed changes in

TABLE I. Parameters obtained from Rietveld refinement of XRD data and experimental data of the samples $L$=Y, $Sm_{0.5}Y_{0.5}$, and $La_{0.5}Y_{0.5}$ with Eq. (5).

| $L$ | Y | $Sm_{0.5}Y_{0.5}$ | $La_{0.5}Y_{0.5}$ |
|---|---|---|---|
| $a$ (Å) | 5.397 | 5.406 | 5.420 |
| $b/\sqrt{2}$ (Å) | 5.374 | 5.392 | 5.402 |
| $c$ (Å) | 5.392 | 5.404 | 5.418 |
| $V$ (Å$^3$) | 221.185 | 222.754 | 224.312 |
| ⟨Mn-O-Mn⟩ (deg) | 160.315 | 160.332 | 160.333 |
| $H_E^0$ (Oe) | 958.050 | 3294.26 | 2246.21 |
| $M_E^0$ (emu/g) | 0.058 | 1.105 | 0.968 |
| $T_{0H}$ (K) | 5.291 | 4.397 | 5.977 |
| $T_{0M}$ (K) | 5.833 | 5.120 | 6.784 |

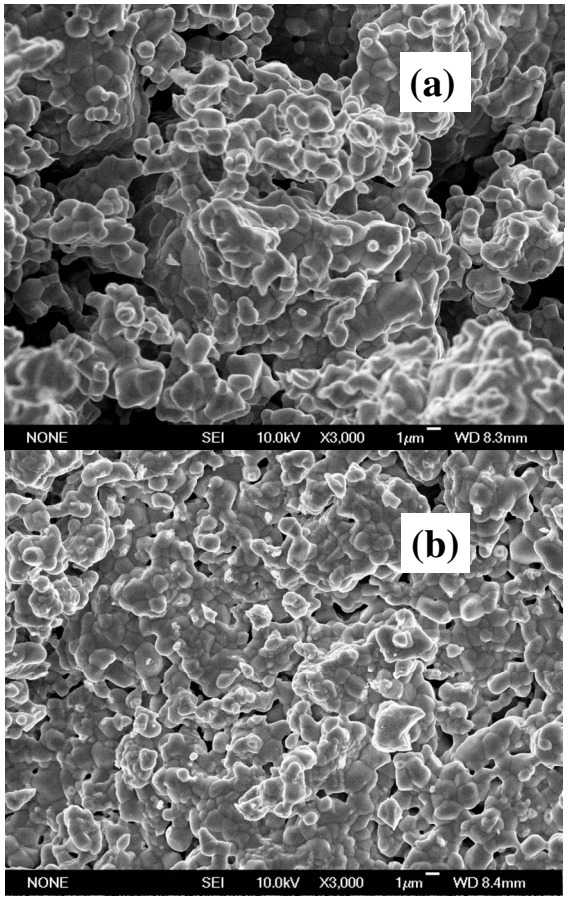


FIG. 2. [(a) and (b)] Scanning electron micrographs for the samples with $L$=Y and $L$=$La_{0.5}Y_{0.5}$, respectively.

EB for the present samples are not due to variation in the grain size, we have performed SEM studies of the samples. Figures 2(a) and 2(b) show SEM images of the typical samples, viz., $Y_{0.5}Sr_{0.5}MnO_3$ and $(La_{0.5}Y_{0.5})_{0.5}Sr_{0.5}MnO_3$, respectively. It is seen that both the samples exhibit similar homogeneity in grain size (~1 $\mu$m) as well as in crystallinity.

### B. Magnetization and spin-glass behavior

In Fig. 3, we have shown the temperature dependent zero field cooled (ZFC) and field cooled (FC) magnetizations $M(T)$ for the $L_{0.5}Sr_{0.5}MnO_3$ ($L$=Y, $Sm_{0.5}Y_{0.5}$, and $La_{0.5}Y_{0.5}$) samples. The ZFC $M(T)$ curves of the samples exhibit sharp peaks at $T_g$=30 K accompanied by a clear bifurcation of ZFC and FC magnetization curves, an indication of spin-glass transition. However, the magnetization of the sample with $L$=$La_{0.5}Y_{0.5}$ shows a different behavior. Around 180 K (say, ~$T_N$), the $M(T)$ curve shows a kink, which is ascribed to the antiferromagnetic ordering transition.[24] At temperature around 50–60 K, both ZFC and FC magnetizations start increasing sharply with decreasing temperature, which shows local onset of ferromagnetic ordering between the clusters. The cusp at temperature $T_{cg}$~40 K shown in the inset of Fig. 3 corresponds to the freezing temperature of these clusters. However, there are domains and spins not belonging to

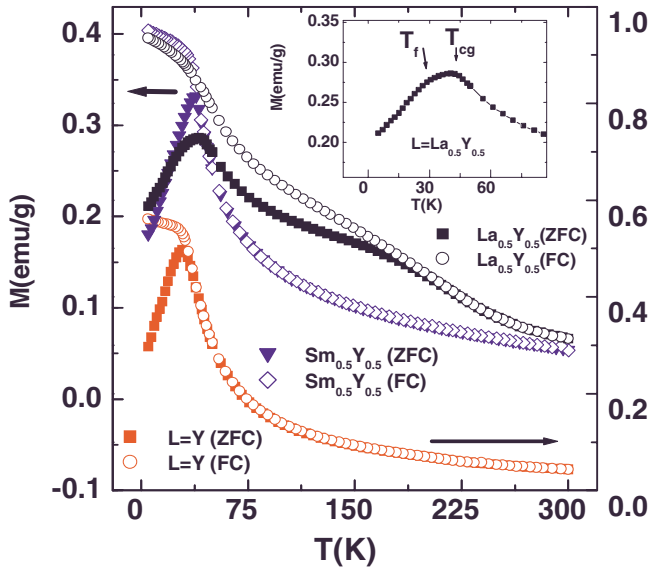


FIG. 3. (Color online) Temperature dependence of ZFC (solid symbols) and FC (open symbols) magnetizations in an applied field of 500 Oe for $L_{0.5}Sr_{0.5}MnO_3$ ($L$=$La_{0.5}Y_{0.5}$, $Sm_{0.5}Y_{0.5}$, and Y) samples.

any clusters which might interact with other spins and form a medium of interaction between the clusters and behave like spin-glass regions.[25] These spins freeze at a temperature corresponding to spin-glass transition temperature $T_f$ (~30 K). Comparing the magnetization curves of the present samples shown in Fig. 3, we can say that the sample with $L$=$La_{0.5}Y_{0.5}$ shows a cluster glass transition at 40 K and a weak spin-glass transition at 30 K, and the samples with $L$=Y and $Sm_{0.5}Y_{0.5}$ show a clear spin-glass transition at 30 K.

To confirm the low temperature glassy magnetic state, we have measured the temperature dependent ac susceptibility ($\chi_{ac}$) of the samples. The temperature dependence of the real part of ac susceptibility ($\chi'$) is shown in Figs. 4(a)–4(c), respectively, for $L$=Y, $Sm_{0.5}Y_{0.5}$, and $La_{0.5}Y_{0.5}$. For the sample $Y_{0.5}Sr_{0.5}MnO_3$, $\chi'$ showed a pronounced peak at around 30 K≈$T_f$ (~$T_g$). A careful investigation of $\chi'(T)$ reveals a small shift of peak position to higher temperature regime for higher driving frequencies. The intensity of the peak also decreases with increasing frequency. Furthermore, for higher temperature, the curves at various frequencies overlap. Such behavior is a characteristic feature of spin glasses and disordered magnetic systems.[25,26] A quantitative measure of the frequency shift of the peak position is represented by the relative shift of the peak temperature $\Delta T_f'/T_f'$ per decade shift in frequency, viz.,

$$K = \frac{\Delta T_f'}{T_f' \Delta \log f}. \quad (1)$$

For $L$=Y, $Sm_{0.5}Y_{0.5}$, and $La_{0.5}Y_{0.5}$, the values of $K$ are ~0.005 39, 0.003 42, and 0.011 83, respectively. For the sake of comparison, the typical $K$ values for spin glasses are 0.02, 0.012, and 0.005, respectively, for $Cd_{0.6}Mn_{0.4}Te$,[27] $Ga_{1-x}Mn_xN$,[28] and Cu:Mn.[25] It is to be noted that the temperature dependence of the in-phase susceptibility $\chi'(T,f)$

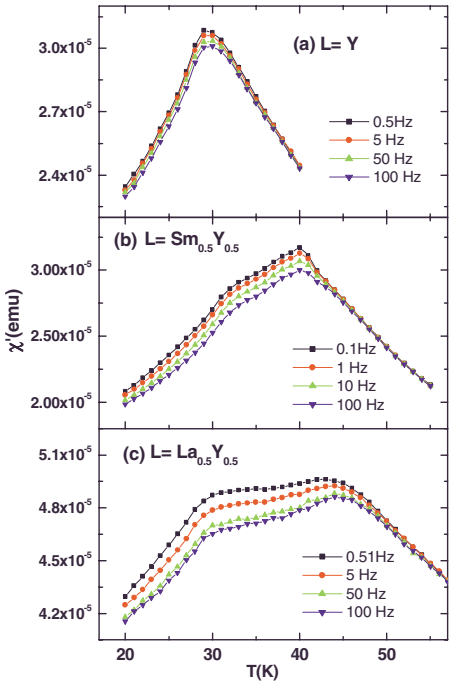


FIG. 4. (Color online) Real part of the ac susceptibility ($\chi$) for (a) $Y_{0.5}Sr_{0.5}MnO_3$, (b) $Sm_{0.25}Y_{0.25}Sr_{0.5}MnO_3$, and (c) $La_{0.25}Y_{0.25}Sr_{0.5}MnO_3$ measured at different frequencies (0.5–100 Hz) of the ac magnetic field.

shows an additional peak around 40–45 K for $L=Sm_{0.5}Y_{0.5}$ and $La_{0.5}Y_{0.5}$. This maximum, however, does not show any uniform frequency dependence, which suggests that the FM ordering is due to the intracluster ferromagnetism around this temperature.

### C. Exchange bias: Cooling field and temperature dependent behavior

It is well known that a spin-disordered interface and/or surface layer is usually formed when a FM particle is embedded in a non-FM matrix or the magnetic particle size is small enough (finite size effect).[29] The exchange bias could also be expected considering coupling between the FM clusters and the SG regions in the intrinsically phase-separated spin and/or cluster glass manganites. To test this argument, we have measured the hysteresis loops of the sample $L_{0.5}Sr_{0.5}MnO_3$ at 2 K under both ZFC and FC conditions. For the ZFC process, the sample was cooled in zero magnetic field from room temperature to 2 K; on the other hand, for the FC process, the sample was cooled in magnetic field (1–6 T) from room temperature to 2 K. Then, the hysteresis loops were measured between ±70 kOe. As shown in Fig. 5, while the ZFC magnetization has a normal hysteresis loop centered at zero field, it is clear that the FC hysteresis loops shift both toward the negative field as well as to the positive magnetization axis. The magnitude of the EB effect observed in the samples is usually compared quantitatively using the following two fields, the exchange-bias field $H_E$ and the coercive field $H_C$ defined, respectively, as[30]

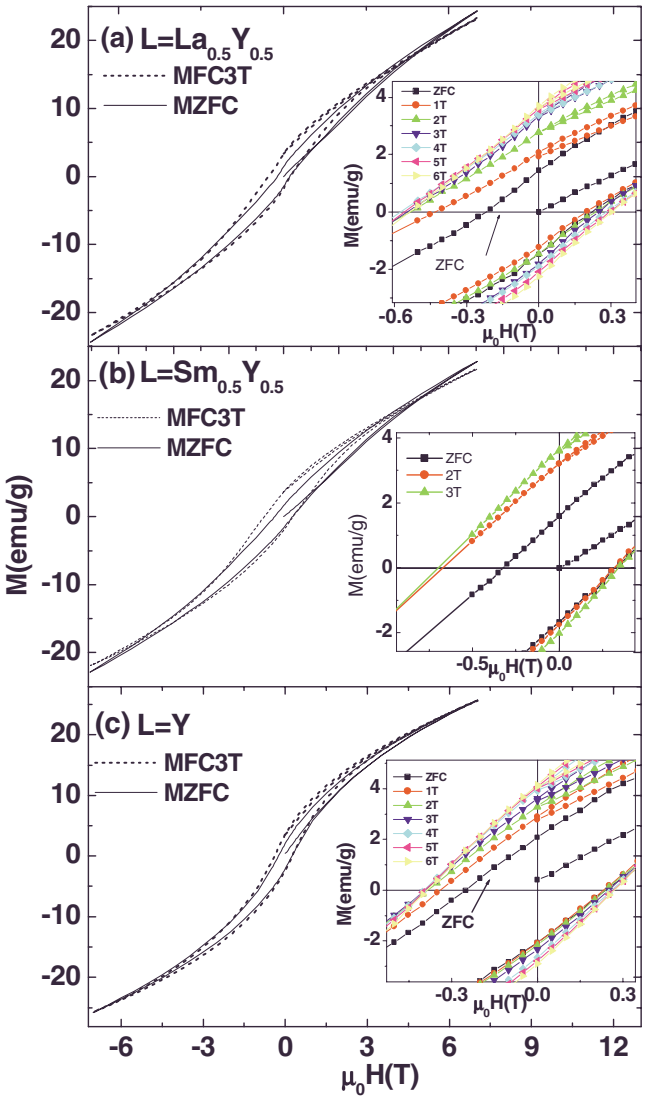


FIG. 5. (Color online) Hysteresis loops of $L_{0.5}Sr_{0.5}MnO_3$, (a) $L=La_{0.5}Y_{0.5}$, (b) $L=Sm_{0.5}Y_{0.5}$, and (c) $L=Y$, at 2 K measured after zero-field cooling (solid line) and field cooling (dashed line) in 30 kOe. Insets show the enlarged view of the low field region.

$$H_C = -\frac{|H_{C1} - H_{C2}|}{2} \quad \text{and}$$

$$H_E = -\frac{(H_{C1} + H_{C2})}{2}, \tag{2}$$

where $H_{C1}$ and $H_{C2}$ are the left and right coercive fields, respectively. Alternatively, the exchange-bias behavior can be seen as an asymmetry in the remanence of the decreasing- and the increasing-field branches of the $M(H)$ loop. This effect is a manifestation of the presence of a unidirectional exchange anisotropy interaction, which drives the FM domains back to the original orientation when the magnetic field is removed. The remanence asymmetry $M_E$ and the magnetic coercivity $M_C$ are usually defined as the "vertical axis" equivalents of $H_E$ and $H_C$, respectively.[31] Figure 6 shows the effect of cooling field on the exchange-bias pa-

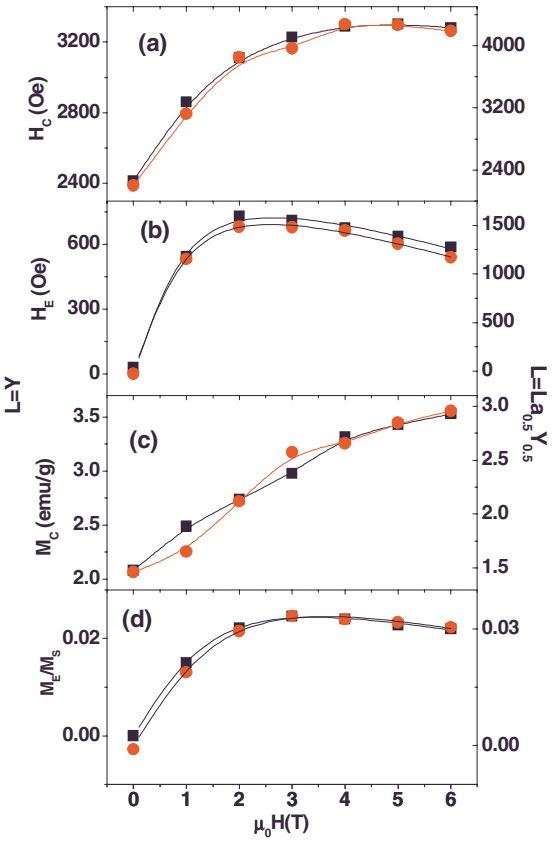


FIG. 6. (Color online) Cooling field dependence of (a) $H_C$, (b) $H_E$, (c) $M_C$, and (d) $M_E$ for $L$=La$_{0.5}$Y$_{0.5}$ (circles) and $L$=Y (squares) at 2 K. For (b) and (d), the solid lines denote the best fitted curves to Eq. (4) described in text. For (a) and (c), the solid lines are guides to the eyes.

rameters $H_E$, $H_C$, $M_E$, and $M_C$ at 2 K for the $L$=Y$_{0.5}$ and La$_{0.5}$Y$_{0.5}$ samples. With the increase of cooling field, the alignment of the moments of FM clusters along a preferential direction is enhanced, which reduces the effect of averaging of the anisotropy due to randomness. All the above mentioned parameters increase sharply with the cooling field up to $H_{\rm cool}$=30 kOe. At a higher cooling field, $M_E$ and $H_C$ tend to saturate but $H_E$ decreases with increasing the cooling field. The decrease in $H_E$ is accompanied by an increase in $M_C$. This suggests that the growth of FM clusters in high cooling field could contribute partly to the decay of $H_E$. However, at high cooling field, not only the alignment degree of the moments of FM clusters is enhanced but the size of FM clusters also increases. As the FM clusters grow, exchange bias is reduced. A schematic diagram for the above discussed behavior of the phase-separated regions present in the samples is shown in Fig. 7 (for simplicity, a two dimensional picture is represented). This effect is qualitatively analogous to FM/AFM thin films, where exchange bias is inversely proportional to the thickness of the FM layer, according to the Meiklejohn and Bean relation,[2] viz.,

$$H_E = -J\frac{S_{\rm AFM}S_{\rm FM}}{\mu_0 t_{\rm FM}M_{\rm FM}}, \tag{3}$$

where $J$ is the exchange integral across the FM/AFM interface per unit area, $S_{\rm AFM}$ and $S_{\rm FM}$ are the interface magnetizations of the antiferromagnet and the ferromagnet, respectively, and $t_{\rm FM}$ and $M_{\rm FM}$ are, respectively, the thickness and magnetization of the FM layer. With increase in cooling field, both denominator and numerator of Eq. (3) increase due to the enhancement of spin alignment, growth of the FM cluster, as well as increase in interface magnetizations [Figs. 7(b) and 7(e)]. However, for strong enough cooling fields, FM clusters become very large, decreasing the overall interface area [Figs. 7(c) and 7(f)] and, hence, $S_{\rm AFM}$ and $S_{\rm FM}$ decrease and $t_{\rm FM}$ increase, which decreases $H_E$ with increasing $H_{\rm cool}$. In their recent work, Niebieskikwiat and Salamon[29] have shown that for $\mu_0 H_{\rm cool} < k_B T$, the $H_{\rm cool}$ dependence of $H_E$ can be expressed by the following relation:

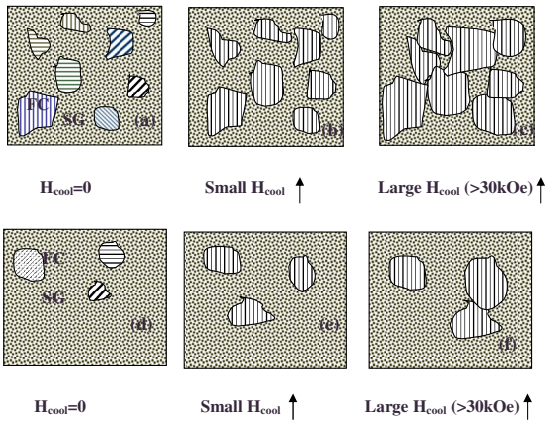


FIG. 7. (Color online) Schematic illustration of the effect of cooling field on the relative proportions of SG, CG, and interface regions: [(a)–(c)] $L$=La$_{0.5}$Y$_{0.5}$, Sm$_{0.5}$Y$_{0.5}$ and [(d)–(e)] $L$=Y samples for $T<T_f$. FC and SG represent ferromagnetic cluster glass and spin-glass regions, respectively.

$$-H_E\alpha\frac{M_E}{M_S}\alpha J_i\left[\frac{J_i\mu_0}{(g\mu_B)}L\left(\frac{\mu H_{\rm cool}}{k_B T_f}\right)+H_{\rm cool}\right], \tag{4}$$

where $L(x)$ is the Langevin function, $k_B$ denotes Boltzmann's constant, and $\mu=N_v\mu_0$. The solid lines in Figs. 6(b) and 6(c) show the best fitted curves to the experimental data with Eq. (4) using an overall scale factor. $J_i$ and $N_v$ are the adjustable parameters. The said fitting indicates quite good agreement of the experimental data with the above model [Eq. (4)]. From this equation, a competition between the exchange interaction and the cooling field becomes quite evident. For small $H_{\rm cool}$, the first term of Eq. (4) usually dominates, and $H_E(<0)$ depends on $J_i^2$. However, for large cooling fields, the second term $(\alpha J)$ becomes important and for $J_i<0$, the absolute value of $H_E$ could decrease or, even more, $H_E$ could change its sign. The exchange constant obtained from the best fit to the experimental data for the present samples was found to be negative $(J_i<0)$. This indicates AFM coupling existing between the FM domains and the AFM host, explaining the tendency of $M_E/M_S$ toward a reduction at high $H_{\rm cool}$. Furthermore, the number of spins per FM droplet obtained are $N_v \approx 21$ (for $L$=Y) and 28 (for $L$=La$_{0.5}$Y$_{0.5}$), which indicate larger FM-CG cluster diameter for $L$=La$_{0.5}$Y$_{0.5}$ than that for the sample with $L$=Y. This feature is also in agreement with the magnetization behavior shown in

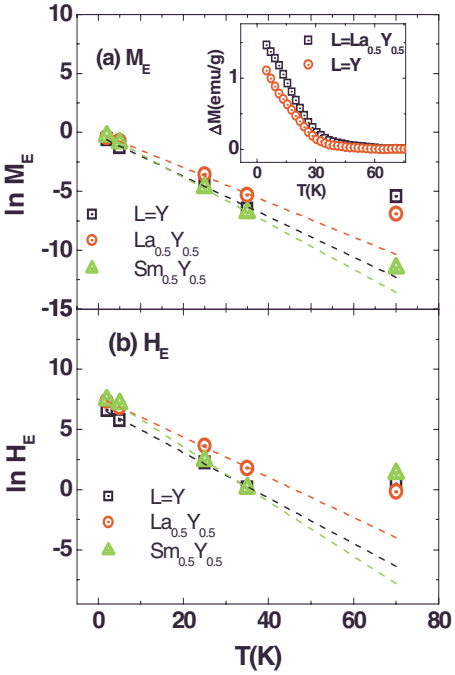


FIG. 8. (Color online) Temperature variation of (a) $\ln(M_E)$ and (b) $\ln(H_E)$ for $L=La_{0.5}Y_{0.5}$, $Sm_{0.5}Y_{0.5}$ and $L=Y$ after field cooling done in 20 kOe. The dashed lines indicate the best fitted lines with Eq. (5) to the experimental data. The inset shows the temperature dependence of magnetic irreversibility $\Delta M=M_{FC}-M_{ZFC}$.

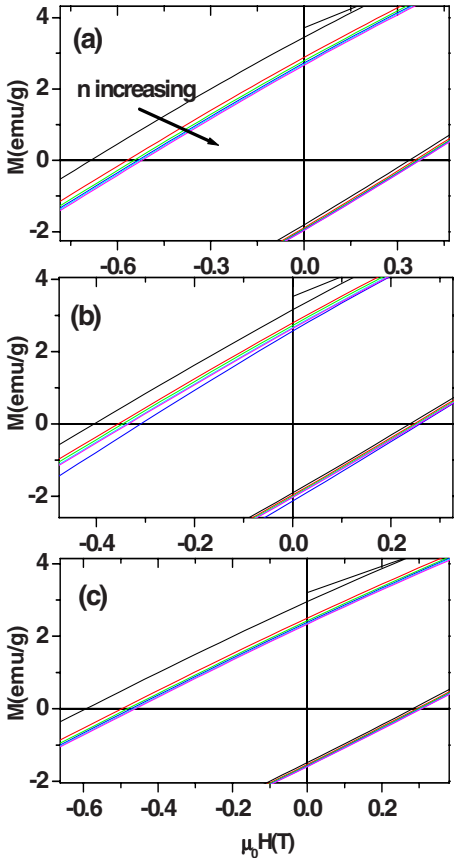


FIG. 9. (Color online) The enlarged view of the central region of the hysteresis loops showing training effect of exchange bias in $L_{0.5}Sr_{0.5}MnO_3$ (a) $L=Sm_{0.5}Y_{0.5}$, (b) $L=Y$, and (c) $L=La_{0.5}Y_{0.5}$, at 2 K. The odd loops, i.e., first, third …, eleventh loops measured at 2 K are shown in the figure after field cooling is done in 30 kOe.

Figs. 3 and 4, as the sample with $L=Y$ shows spin-glass-like behavior and for $L=La_{0.5}Y_{0.5}$, a mixed cluster glass (CG) and SG behavior is observed at low temperature.

It is also to be noted that with increasing $H_{cool}$, the magnetic coupling (Zeeman coupling) between the spins at the interfaces between the FM clusters and the surrounding non-FM matrix increases as well, tending to orient them along the field direction.[29,30] At around $T=2$ K, for high enough fields, such coupling may compete with the mixed magnetic interactions within the system, overcoming the exchange coupling at the interface between CG and SG regions. However, the variation of $H_E$ with cooling field (Fig. 6) indicates that the interface between the FM-CG and disordered SG is smooth and it is further suggested[31,32] that for such a smooth interface, the strength of EB is greater than the Zeeman coupling. Both the growth of FM clusters and the reduction of the spin disorder at the interfaces eventually weaken the exchange bias.

To reveal the origin of exchange bias in the present mixed valence samples, the temperature dependence of exchange bias parameters has also been studied. For such measurements, the sample was cooled down from room temperature to the measuring low temperature with an applied field $H_{cool}=20$ kOe. Once the measuring temperature was reached, the magnetization loop was measured between $\pm 70$ kOe. This process was repeated for every measuring temperature. As shown in Fig. 8, for the present samples, with increasing temperature, both $M_E$ and $H_E$ decrease sharply, in correspondence with the freezing temperature $T_f$. The temperature evolution of $H_E$ is typical for the exchange-biased systems with FM/SG interfaces.[33] As the sample is cooled through $T_N \sim 180$ K with an applied magnetic field, the moments of FM clusters line up with the field, while the SG spins remain random. When cooling to $T \sim T_f$, in the presence of a magnetic field, the SG spins next to the FM clusters arrange along a specific direction due to the exchange interaction at the FM/SG interface. In turn, below $T_f$, the SG spins at the interface exert a microscopic torque on the FM spins to keep them in their original direction. Thus, the magnetization loop is shifted along the field axis, i.e., exchange bias appears. In addition, the magnetization shift $M_E$ is also observed at different temperatures, as shown in Fig. 8. The magnetic frustration is known to lead to the exponential decay of $H_E$ and $H_C$ as has been observed in the multilayer systems containing amorphous or spin-glass layer.[34,35] Thus, we can fit the observed $H_E$ and $H_C$ with the equation

$$H_E = H_E^0 \exp(-T/T_0), \tag{5}$$

where $H_E^0$ is the extrapolation of $H_E$ at 0 K and $T_0$ is a constant. The corresponding best fitted parameters are given in Table I. When the temperature is above $T_f$, displacement of the hysteresis loop disappears and $H_E$ becomes nearly zero. The increase of more than 1 order of magnitude of $M_E$ and

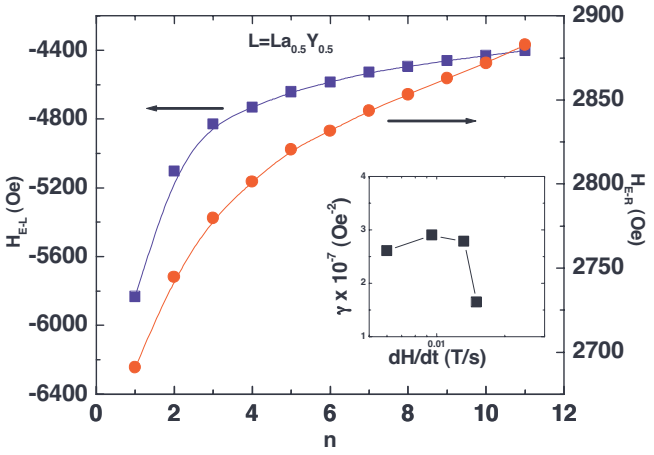


FIG. 10. (Color online) The number of field cycles ($n$) dependence of right and left field branches of coercivity for the $La_{0.5}Y_{0.5}Sr_{0.5}MnO_3$ sample at 2 K after field cooling is done in 30 kOe.

$M_C$ below $T_f$ is due to the enhancement of the magnetic irreversibility induced by the freezing of the spin-glass regions. The magnetic irreversibility ($\Delta M = M_{FC} - M_{ZFC}$) also shows a similar temperature dependent behavior [Fig. 8(a) inset]. The value of $\Delta M$ remains almost zero around $T_f$ and increases sharply as the temperature is lowered further. This indicates that initial blocking of quite a small number of interfaces occurs at $T_N$ and dominant contribution to the low temperature $M_E$, however, comes from the domains around $T_f \sim 30$ *K*. The existence of low $T_f$ EB effect has also been observed in some other different systems, where the EB effects have been attributed to glasslike phases occurring in spin-disordered surfaces around the ordered particles.[5,31–33]

### D. Training effect

In exchange bias systems, as the material is continuously field cycled, a gradual decrease of the anisotropy interaction is commonly found, the so-called training effect.[34–38] As a result, both $H_E$ and $H_C$ fields decrease with increasing loop index number. For the present samples, the consecutive hysteresis loops were measured continuously at $T=2$ K after field cooling in 30 kOe. Figure 9 shows the expansion of the low field region (only loops with index number $n=1$, 3, 5, 7, 9, and 11 are shown). It is obvious that the training effect is present in our sample. The relaxation of the remanence asymmetry is evident and, as shown by the evolution of $H_E(M_E)$ with $n$ (Fig. 10), this relaxation is particularly important between the first and second loops, where $H_E(M_E)$ is seen to fall sharply. From Fig. 9, it appears that this shift is only observed around the left branch of the hysteresis loop; however, in practice, it was found that both branches showed field shifts. Figure 10 shows the training effect on the left ($H_{E\text{-}L}$) and right ($H_{E\text{-}R}$) coercive field branches individually for the $L=Y_{0.5}La_{0.5}$ sample. Although for the first few cycles ($n \leqslant 4$) $H_{E\text{-}L}$ rises faster than $H_{E\text{-}R}$, for the later cycles ($n > 4$), $H_{E\text{-}L}$ saturates and $H_{E\text{-}R}$ keeps on increasing almost linearly. Since the variation of $H_{E\text{-}R}$ is much smaller than that of $H_{E\text{-}L}$, it appears that $H_{E\text{-}R}$ remains almost constant throughout the training procedure. The fact that field cycling appears to affect $H_{E\text{-}L}$ more strongly than $H_{E\text{-}R}$ is suggestive of thermal activation in the FM region being dominant in the field-training response.[39] Domains in the SG/AFM regions may get switched due to thermal activation along each branch of the loop. The number of such reversals ought to be the same on either branch because it is only sensitive to the ferromagnetic magnetization, and this has the same magnitude in both directions of the field sweep. However, the ferromagnetic region, which is not strongly biased, experiences a different magnitude of field during the forward and reverse branches, since the loop is offset from $H=0$. The number of thermally activated reversals in this set of weakly biased regions will be greater for the reverse branch of the loop where the field magnitude is larger. Any associated changes in the SG/AFM regions would therefore be larger near $H_{E\text{-}L}$ compared to $H_{E\text{-}R}$.

It is often found experimentally that the relationship between $H_E(M_E)$ and $n$ can be expressed by a simple power law:

$$\mu_0 H_E - \mu_0 H_{E_\infty} = \frac{\kappa}{\sqrt{n}}. \tag{6}$$

Here, $H_{E\infty}$ is the exchange-bias field in the limit of infinite loops and $\kappa$ is the sample-dependent constant.[29,38] Figure 11 (inset) shows the best fitted curves of the experimental data (both $H_E$ and $M_E$ data for $n>1$) with Eq. (6). The fitted curves show satisfactory agreement with the experimental data and the corresponding fitting parameters are given in Table II. Although the power-law decay of exchange bias has widely been observed, its origin still remains unexplained. Equation (6) is, however, applicable only for $n>1$. Recently, Binek *et al.*[38] considered the training effect in FM/AFM heterostructures in the framework of nonequilibrium thermodynamics. It was proposed that consecutively cycled hysteresis loops of the FM top layer trigger the spin configurational relaxation of the AFM interface magnetization toward equilibrium and a recursive formula can be obtained describing $n$ dependence of $H_E(M_E)$.[38] This relation can be written as

$$H_E(n+1) - H_E(n) = -\gamma_H [H_E(n) - H_{E\infty}]^3, \tag{7}$$

where $\gamma_H$ is a sample-dependent constant. The analytical approach is confirmed by experimental results obtained recently on a NiO(001)/Fe(110) heterostructure and a Co/CoO exchange-biased bilayer.[38,40] Using the initial value of $H_E(1)$, obtained experimentally, $\gamma$, and $H_{E\infty}$, as given in Table II, the theoretical data of $H_E$ are calculated (solid circles in Fig. 11) from the implicit sequence in Eq. (7). Similarly, the theoretical data of $M_E$ (solid squares in Fig. 11) are obtained with $M_E(1)$, $\gamma_M$, and $M_{E\infty}$ as shown in Table II. It is seen that both the theoretical values of $H_E$ and $M_E$ are well coincident with the corresponding experimental results. The training effect can be explained in terms of the demagnetization of the non-FM surface regions.[36,41] As the FM domain switches back and forth under the influence of the applied field, a relaxation of the surface spin configuration toward the equilibrium is induced due to the surface drag of the exchange interaction. This is particularly relevant for the

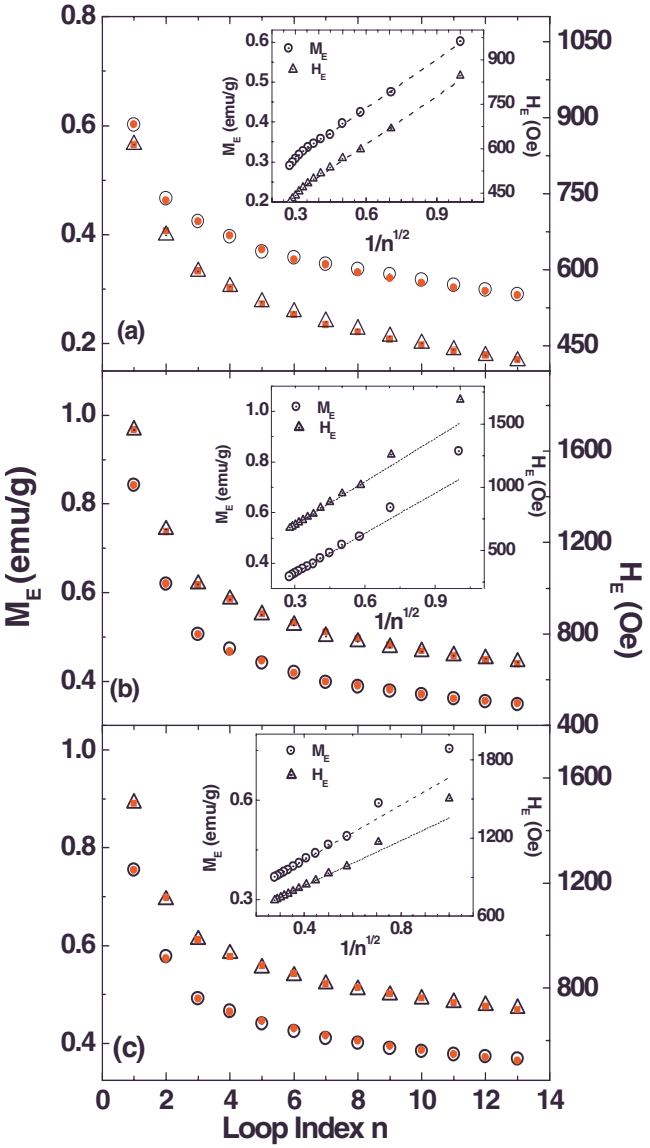


FIG. 11. (Color online) The number of field cycles ($n$) dependence of $H_E$ and $M_E$ (open symbols) for $L_{0.5}Sr_{0.5}MnO_3$, (a) $L=Sm_{0.5}Y_{0.5}$, (b) $L=Y$, and (c) $L=La_{0.5}Y_{0.5}$, at 2 K. The solid symbols and line correspond to the data generated from the recursive sequence [(Eq. (7))] as described in the text. Insets show the best fits with Eq. (6) to the data for $n>1$.

spin-glass-like phase observed in the present system of our investigation, since when the applied field consecutively cycles, some of the frozen SG spins along the cooling field direction may change their directions and fall into other metastable configurations, which would decrease the strength of exchange coupling at the interfaces. Therefore, the observed training effect in manganites can be interpreted well with the spin configurational relaxation model [Eq. (7)].

### E. Magnetic-field step size dependence

The EB phenomena have been reported to be very sensitive to the field sweep rate variation[42–45] i.e., $dH/dt$, the bias field decreases and the coercive field increases above a field sweep rate of a few T/s. The observed reduction of exchange bias at high frequencies correlates with a magnetization reversal asymmetry at low field sweep rates. Recently, Ouyang *et al.*[46] have shown that the effect of the variation of the magnetic-field step size ($\Delta H$) in a SQUID magnetometer is similar to that of the magnetic-field sweep rate in a vibrating sample magnetometer, which suggests that such $\Delta H$ variation effects can be compared well to the $dH/dt$ results.

TABLE II. Parameters obtained from the best-fit curves of the experimental data of the samples $L=Y$, $Sm_{0.5}Y_{0.5}$, and $La_{0.5}Y_{0.5}$ with Eqs. (6) and (7).

| $L$ | Y | $Sm_{0.5}Y_{0.5}$ | $La_{0.5}Y_{0.5}$ |
|---|---|---|---|
| $H_{E_\infty}$ (Oe)[a] | 287.021 | 360.167 | 484.645 |
| $M_{E_\infty}$ (emu/g)[a] | 0.186 | 0.202 | 0.252 |
| $H_{E_\infty}$ (Oe)[b] | 152.96 | 110.29 | 286.13 |
| $M_{E_\infty}$ (emu/g)[b] | 0.083 | 0.077 | 0.156 |
| $\gamma_H$ ($10^{-7}$ Oe$^{-2}$)[b] | 7.461 | 1.706 | 2.882 |
| $\gamma_M$ (emu/g)$^{-2}$ [b] | 1.275 | 0.753 | 1.230 |

[b]From Eq. (6).

Figures 12(a) and 12(b) show the step size dependence of the absolute values of $H_C$ and $H_E$, respectively, for the sample $L=La_{0.5}Y_{0.5}$. It has been observed that an increase in the applied field step size enhances the value of coercivities $H_C$ considerably. On the other hand, $H_E$ first increases and then decreases with further increase of $\Delta H$. This kind of behavior is generally attributed to the thermally activated magnetization reversal mechanism.[47] This logarithmic dependence of coercivity on magnetic-field sweep rate can be explained using the following phenomenological model:[48]

$$H_C = \frac{kT}{V^* M_S}\left[\ln\left(\frac{dH}{dt}\right) + \ln\left(\tau(H=0)\ln 2\frac{V^* M_S}{kT}\right)\right] - H_E, \tag{8}$$

where $M_S$ is the saturation magnetization, $V^*$ is the Barkhausen volume, i.e., the characteristic volume which reverses magnetization during a wall jump, and $\tau_{\omega 0}$ is the relaxation time, i.e., time to overcome the activation energy barrier in the absence of an applied field. The values of $(dH/dt)$ were calculated numerically following the procedure shown by Ouyang *et al.*[46] Figure 12(c) shows that the experimental data are in good agreement with Eq. (8). The fitting parameters $V^*$ and $\tau_{\omega 0}$, obtained from fitting the experimental data to Eq. (8), are $(2\ \text{nm})^3$ and $7.6\times 10^9$ s, respectively. The value of $V^*$ is much smaller than the sample's average grain size; this suggests that there is a strong intergrain interaction present in the system.[49]

The effect of field step size for the present samples was also studied. A dynamical broadening of the hysteresis loops were observed for increased field steps and (hence sweep

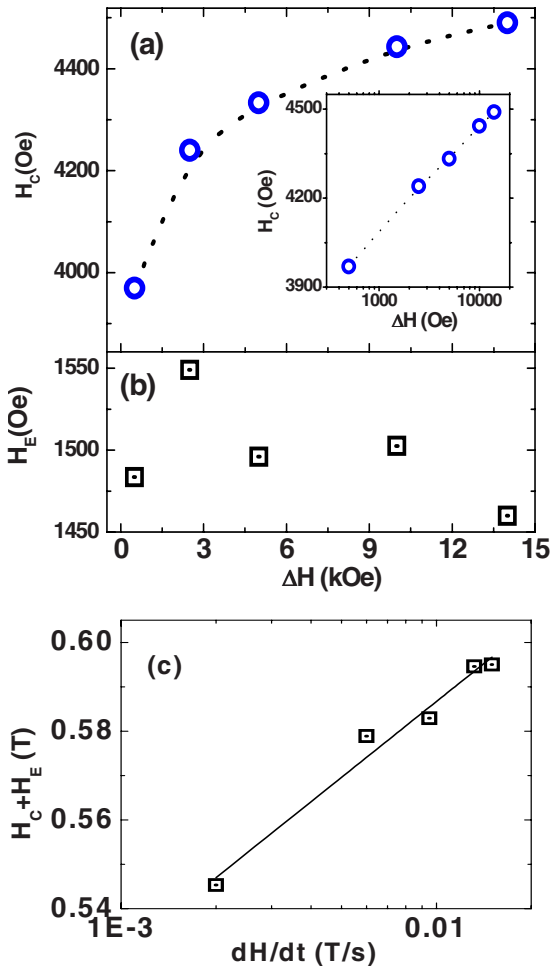


FIG. 12. (Color online) The applied field step size ($\Delta H$) dependence of (a) $H_E$ and (c) $H_C$ for $La_{0.5}Y_{0.5}Sr_{0.5}MnO_3$ at 2 K after field cooling is done in 30 kOe and the dashed lines are guides to the eyes. (c) Variation of $(H_C+H_E)$ with calculated sweep rate $(dH/dt)$. The solid line shows the best fit to the data with Eq. (8), discussed in text.

rate). The variation of the parameter $\gamma_H$ [Eq. (7)] with $dH/dt$ is shown in Fig. 10 (inset); this is in agreement with the model explained by Sahoo *et al.* recently.[42]

From the above results, we can say that the nature of exchange-bias phenomena in the present $L_{0.5}Sr_{0.5}MnO_3$ ($L$ = Y, $Sm_{0.5}Y_{0.5}$, and $La_{0.5}Y_{0.5}$) samples are qualitatively similar. However, from Tables I and II, we find that the values of various exchange field parameters are larger by 1 order of magnitude for $L=Sm_{0.5}Y_{0.5}$ and $La_{0.5}Y_{0.5}$ compared to those of the $L$=Y sample. This can be attributed to the relatively smaller number of FM clusters for the sample with $L$=Y [Fig. 7(d)]. Since this sample has a larger cation size disorder, $\sigma^2 = \sigma^2 = \Sigma x_i r_i^2 - r_A^2$),[50] than those of $Sm_{0.5}Y_{0.5}$ and $La_{0.5}Y_{0.5}$, the double exchange mechanism is relatively weaker. At higher temperature, the overall order is AFM and, therefore, large FM cluster formation is rather less probable. However, the values of $\sigma^2$ for the samples with $L$ $=Sm_{0.5}Y_{0.5}$ and $La_{0.5}Y_{0.5}$ are smaller and, hence, they have a larger number of FM clusters [Fig. 7(a)], resulting to the formation of greater interface regions (and hence greater $H_E$).

## IV. CONCLUSION

In conclusion, from the present detailed low temperature magnetic measurements, we provided evidence of intrinsic interface exchange-bias effect in a bulk manganite system having FM cluster glass and disordered spin-glass interfaces. It is observed that the exchange field, coercivity, and remanence asymmetry strongly depend on the cooling field strength for these typical mixed valent manganite samples. The observed behavior has been explained by taking into account the strength of exchange coupling between the FM and the SG regions and their relative proportions present in the system. It was found that with the variation of the cooling field, different frozen magnetic configurations of the system are selected, allowing the tuning of $H_E$, $H_C$, and $M_E$ over their wide ranges. Continuous field cycling (i.e., training effect) was found to affect strongly on only one branch of the magnetization loop and could be explained by a distribution of fields acting on the FM regions. Increase in applied field step size increases the coercive field of the loops almost exponentially. The observed training effect of the exchange bias can also be described with the same relaxation model used for other classical exchange-bias systems, indicating a unique mechanism for exchange anisotropy.

## ACKNOWLEDGMENTS

The authors S. K. and S. T. gratefully acknowledge the Council for Scientific and Industrial Research (CSIR), India for financial support. This work was also partially supported by the National Science Council of Taiwan under Grant No. NSC96–2112–M110–001.

*Corresponding author; sspbkc@iacs.res.in

[1] R. L. Stamps, J. Phys. D **33** R247 (2000).
[2] W. H. Meiklejohn and C. P. Bean, Phys. Rev. **102**, 1413 (1956).
[3] B. Martínez, X. Obradors, L. Balcells, A. Rouanet, and C. Monty, Phys. Rev. Lett. **80**, 181 (1998).
[4] V. Skumryev, S. Stoyanov, Y. Zhang, G. Hadjipanayis, D. Givord, and J. Nogués, Nature (London) **423**, 850 (2003).
[5] J. S. Kouvel, J. Phys. Chem. Solids **24**, 795 (1963).
[6] J. Nogués and I. K. Schuller, J. Magn. Magn. Mater. **192**, 203 (1999).
[7] S. G. E. te Velthuis, G. P. Felcher, J. S. Jiang, A. Inomata, C. S. Nelson, A. Berger, and S. D. Bader, Appl. Phys. Lett. **75**, 4174 (1999).
[8] D. L. Peng, K. Sumiyama, T. Hihara, S. Yamamuro, and T. J. Konno, Phys. Rev. B **61**, 3103 (2000).
[9] M. Ali, P. Adie, C. H. Marrows, D. Greig, B. J. Hickey, and R. L.

Stamps, Nat. Mater. **6**, 70 (2007).
[10] W. J. Antel, Jr., F. Perjeru, and G. R. Harp, Phys. Rev. Lett. **83**, 1439 (1999).
[11] H. Ohldag, A. Scholl, F. Nolting, E. Arenholz, S. Maat, A. T. Young, M. Carey, and J. Stöhr, Phys. Rev. Lett. **91**, 017203 (2003).
[12] M. Gruyters and D. Riegel, Phys. Rev. B **63**, 052401 (2000).
[13] S. Jin, T. H. Tiefel, M. McCormack, R. A. Fastnacht, R. Ramesh, and L. H. Chen, Science **264**, 413 (1994).
[14] E. Dagotto, *Nanoscale Phase Separation and Colossal Magnetoresistance* (Springer-Verlag, Berlin, 2003).
[15] A. J. Millis, P. B. Littlewood, and B. I. Shraiman, Phys. Rev. Lett. **74**, 5144 (1995).
[16] S. Murakami and N. Nagaosa, Phys. Rev. Lett. **90**, 197201 (2003).
[17] Y. Tokura and N. Nagaosa, Science **288**, 462 (2000); Nature (London) **399**, 560 (1999).
[18] R. Mathieu, D. Akahoshi, A. Asamitsu, Y. Tomioka, and Y. Tokura, Phys. Rev. Lett. **93**, 227202 (2004).
[19] Y. Tokura, Rep. Prog. Phys. **69**, 797 (2006).
[20] W. Wu, C. Israel, N. Hur, S. Park, S. W. Cheong, and A. D. Lozanne, Nat. Mater. **5**, 881 (2006).
[21] S. A. Wolf, D. D. Awschalom, R. A. Buhrman, J. M. Daughton, S. von Molnár, M. L. Roukes, A. Y. Chtchelkanova, and D. M. Treger, Science **294**, 1488 (2001).
[22] P. M. Woodward, T. Vogt, D. E. Cox, A. Arulraj, C. N. Rao, P. Karen, and A. K. Cheetham, Chem. Mater. **10**, 3652 (1998).
[23] Sadia Manzoor, M. Vopsaroiu, G. Vallejo-Fernandez, and K. O'Grady, J. Appl. Phys. **97**, 10K118 (2005).
[24] F. Damay, A. Maignan, C. Martin, and B. Raveau, J. Appl. Phys. **81**, 1372 (1997).
[25] J. A. Mydosh, *Spin Glasses: An Experimental Introduction* (Taylor & Francis, London, 1993).
[26] R. H. Kodama, A. E. Berkowitz, E. J. McNiff, and S. Foner, Phys. Rev. Lett. **77**, 394 (1996).
[27] A. Mauger, J. Ferre, M. Ayadi, and P. Nordblad, Phys. Rev. B **37**, 9022 (1988).
[28] S. Dhar, O. Brandt, A. Trampert, K. J. Friedland, Y. J. Sun, and K. H. Ploog, Phys. Rev. B **67**, 165205 (2003).
[29] D. Niebieskikwiat and M. B. Salamon, Phys. Rev. B **72**, 174422 (2005).
[30] C. Leighton, J. Nogués, H. Suhl, and I. K. Schuller Phys. Rev. B **60**, 12837 (1999).
[31] C. Leighton, J. Nogués, B. J. Jösson-Akerman, and I. K. Schuller, Phys. Rev. Lett. **84**, 3466 (2000).
[32] Lucia Del Bianco, Dino Fiorani, Alberto M. Testa, Ennio Bonetti, and Luca Signorini, Phys. Rev. B **70**, 052401 (2004); B. Martínez, X. Obradors, Ll. Balcells, A. Rouanet, and C. Monty, Phys. Rev. Lett. **80**, 181 (1998); M. Gruyters, Phys. Rev. Lett. **95**, 077204 (2005).
[33] V. Korenivski, R. B. van Dover, Y. Suzuki, E. M. Gyorgy, J. M. Phillips, and R. J. Felder, J. Appl. Phys. **79**, 5926 (1996).
[34] B. Aktas, Y. Öner, and H. Z. Durusoy, J. Magn. Magn. Mater. **119**, 339 (1993).
[35] Yan-kun Tang, Young Sun, and Zhao-hua Cheng, Phys. Rev. B **73**, 012409 (2006).
[36] J. Keller, P. Miltényi, B. Beschoten, G. Güntherodt, U. Nowak, and K. D. Usadel, Phys. Rev. B **66**, 014431 (2002).
[37] R. K. Zheng, G. H. Wen, K. K. Fung, and X. X. Zhang, Phys. Rev. B **69**, 214431 (2004).
[38] Ch. Binek, Phys. Rev. B **70**, 014421 (2004).
[39] L. Wee, R. L. Stamps, L. Malkinski, and Z. Celinski, D. Skrzypek, Phys. Rev. B **69**, 134425 (2004).
[40] A. Hochstrat, Ch. Binek, and W. Kleemann, Phys. Rev. B **66**, 092409 (2002); A. Hoffmann, Phys. Rev. Lett. **93**, 097203 (2004).
[41] M. Hennion, F. Moussa, G. Biotteau, J. Rodríguez-Carvajal, L. Pinsard, and A. Revcolevschi, Phys. Rev. B **61**, 9513 (2000).
[42] S. Sahoo, S. Polisetty, Ch. Binek, and A. Berger, J. Appl. Phys. **101**, 053902 (2007).
[43] J. Camarero, Y. Pennec, J. Vogel, M. Bonfim, S. Pizzini, M. Cartier, F. Ernult, F. Fettar, and B. Dieny, Phys. Rev. B **64**, 172402 (2001).
[44] J. Appl. Phys. **101** 09E513 (2007).
[45] Haiwen Xi, Scott Franzen, and Robert M. White, J. Appl. Phys. **101**, 09E513 (2007).
[46] Z. W. Ouyang, V. K. Pecharsky, K. A. Gschneidner, Jr., D. L. Schlagel, and T. A. Lograsso, Phys. Rev. B **76**, 134406 (2007).
[47] L. Wee, R. L. Stamps, L. Malkinski, Z. Celinski, and D. Skrzypek, Phys. Rev. B **69**, 134425 (2004).
[48] Gregory Malinowski, Sebastiaan van Dijken, Maciej Czapkiewicz, and Tomasz Stobiecki, Appl. Phys. Lett. **90**, 082501 (2007).
[49] C. Gao, Z. S. Shan, R. Malmhäll, Y. Liu, H. J. Richter, A. Barney, G. C. Rauch, and D. J. Sellmyer, J. Appl. Phys. **81**, 3928 (1997).
[50] L. M. Rodriguez-Martinez and J. P. Attfield, Phys. Rev. B **54**, R15622 (1996).